

$\eta'K$ puzzle of B meson decays and new physics effects in the general two-Higgs-doublet model

Zhenjun Xiao^{(1,2) *}, Chong Sheng Li⁽¹⁾

1. Department of Physics, Peking University, Beijing, 100871, People's Republic of China
 2. Department of Physics, Henan Normal University, Xinxiang, Henan, 453002, People's Republic of China

Kuang-Ta Chao

CCAST(World Laboratory), P.O.Box 8730, Beijing 100080, People's Republic of China
 and Department of Physics, Peking University, Beijing, 100871, People's Republic of China
 (January 13, 2019)

Abstract

we calculate the new physics contributions to seven measured decays $B \rightarrow \pi^+\pi^-$, $K\pi$ and $K\eta'$ in the general two-Higgs-doublet model (Model III). Within the considered parameter space, we find that: (a) the CLEO/BaBar measurement of $B \rightarrow \pi^+\pi^-$ decay prefers a small $F_0^{B\pi}(0)$: $F_0^{B\pi}(0) = 0.25 \pm 0.03$; (b) the new physics enhancements to the penguin-dominated $B \rightarrow K\pi$ and $B \rightarrow K\eta'$ decays are significant in size, $\sim (40 - 70)\%$ *w.r.t* the standard model predictions; and (c) the new physics enhancements can boost the branching ratios $\mathcal{B}(B \rightarrow K^+\eta')$ and $\mathcal{B}(B \rightarrow K^0\eta')$ to be consistent with the data within one standard deviation, and hence lead to a simple and plausible new physics interpretation for the $\eta'K$ puzzle.

PACS numbers: 13.25.Hw, 12.15.Ji, 12.38.Bx, 12.60.Fr

*E-mail: zxiao@ibm320h.phy.pku.edu.cn

One of the main objectives of B experiments is to probe for possible effects of new physics beyond the standard model (SM). Precision measurements of B meson system can provide an insight into very high energy scales via the indirect loop effects of new physics. The B system therefore offers a complementary probe to the search for new physics at other hadron colliders [1,2].

Up to now, CLEO, BaBar and Belle Collaboration [3–6] have observed fourteen $B_{u,d}$ meson two-body charmless hadronic decay modes

$$B \rightarrow \pi^\pm \pi^\mp, K\pi, K\eta', \rho^\pm \pi^\mp, \rho^0 \pi^\pm, \omega \pi^\pm, K^* \eta, K^{*\pm} \pi^\mp, \phi K^\pm. \quad (1)$$

The experimental measures are generally consistent with the theoretical predictions based on the effective Hamiltonian with generalized factorization [7,8], with an exception of the so-called $\eta' K$ puzzle: the $B \rightarrow K\eta'$ decay rates are much larger than that expected in the SM [3].

The unexpectedly large branching ratios of $B \rightarrow K\eta'$ was firstly reported in 1997 by CLEO [9], and confirmed very recently by CLEO and BaBar [3,5]: $\mathcal{B}(B \rightarrow K^+ \eta') = (75 \pm 10) \times 10^{-6}$ (average of the CLEO and BaBar result), and $\mathcal{B}(B \rightarrow K^0 \eta') = (89 \pm 16 \pm 9) \times 10^{-6}$ (CLEO). The $K\eta'$ signal is large and stable, and clearly much larger than the SM predictions $\mathcal{B}(B \rightarrow K\eta') = (20 - 50) \times 10^{-6}$ as given in Refs. [7,10,11]. In order to accommodate the data, one may need an additional contribution unique to the η' meson in the framework of the SM, or enhancements from new physics models beyond the SM to explain the $B \rightarrow K\eta'$ puzzle [12].

In a previous paper [11], we considered the second possibility and calculated the new physics effects on the branching ratios of seventy six $B \rightarrow h_1 h_2$ decay modes in the general two-Higgs-doublet models (2HDM's) [13,14], and found that the new physics enhancement to the penguin-dominated decay modes can be significant. In this letter, we focus on seven $B \rightarrow PP$ decays (where P refers to the light pseudo-scalar mesons) whose branching ratios have already been measured. We firstly find the constraint on the form factor $F_0^{B\pi}(0)$ from the measured $B \rightarrow \pi^\pm \pi^\mp$ decay rate, and then check the consistency between the theoretical predictions and the data for the four $B \rightarrow K\pi$ decay modes after including the new physics contributions in model III: the third type of two-Higgs-doublet models [13,14]. We finally calculate the new physics enhancements to the $B \rightarrow K\eta'$ decays and study the effects of major uncertainties.

On the theory side, one usually uses the low-energy effective Hamiltonian with generalized factorization [15,16,7,8] to calculate the two-body charmless B meson decays. For the inclusive three-body decays $b \rightarrow s\bar{q}q$ with $q \in \{u, d, s\}$ the effective Hamiltonian can be written as [7],

$$\mathcal{H}_{eff}(\Delta B = 1) = \frac{G_F}{\sqrt{2}} \left\{ \sum_{j=1}^2 C_j \left(V_{ub} V_{us}^* Q_j^u + V_{cb} V_{cs}^* Q_j^c \right) - V_{tb} V_{ts}^* \left[\sum_{j=3}^{10} C_j Q_j + C_g Q_g \right] \right\}, \quad (2)$$

where the operator basis contains the current-current operators $Q_{1,2}$, the QCD penguin operators Q_{3-6} , the electroweak penguin operators Q_{9-10} and the chromo-magnetic dipole operator Q_g , the explicit expressions can be found easily for example in Ref. [7]. For $b \rightarrow d\bar{q}q$ decays, one simply makes the replacement $s \rightarrow d$.

Following Ref. [7], we also neglect the effects of the electromagnetic penguin operator $Q_{7\gamma}$, and do not consider the effect of the weak annihilation and exchange diagrams. The

coefficients C_i in Eq.(2) are the well-known Wilson coefficients. Within the SM and at scale M_W , the Wilson coefficients $C_1(M_W), \dots, C_{10}(M_W)$ at next-to-leading logarithmic order (NLO) and $C_g(M_W)$ at leading logarithmic order (LO) have been given for example in Ref. [15].

In a recent paper [17], Chao *et al.* studied the decay $b \rightarrow s\gamma$ in model III by assuming that only the couplings $\lambda_{tt} = |\lambda_{tt}|e^{i\theta_t}$ and $\lambda_{bb} = |\lambda_{bb}|e^{i\theta_b}$ are non-zero¹. They found that the constraint on M_{H^+} imposed by the CLEO data of $b \rightarrow s\gamma$ can be greatly relaxed by considering the phase effects of λ_{tt} and λ_{bb} . From the studies of Refs. [2,17], we know that for model III the parameter space

$$\begin{aligned} \lambda_{ij} &= 0, \quad \text{for } ij \neq tt, \text{ or } bb, \\ |\lambda_{tt}| &= 0.3, \quad |\lambda_{bb}| = 35, \quad \theta = (0^0 - 30^0), \quad M_{H^+} = (200 \pm 100) \text{ GeV}, \end{aligned} \quad (3)$$

are allowed by the available data, where $\theta = \theta_{bb} - \theta_{tt}$. In this letter, we calculate the new physics contributions to seven B meson decay modes in the Chao-Cheung-Keung (CCK) scenario of model III [17]. Since the new physics corrections on the branching ratios of two-body charmless hadronic $B_{u,d}$ decays in models I and II are small in magnitude [11], we do not consider the cases of models I and II in this letter.

Following the same procedure as in the SM, it is straightforward to calculate the new γ -, Z^0 - and gluonic penguin diagrams induced by the exchanges of charged-Higgs bosons appeared in model III [11]. After taking into account the new physics (NP) contributions, the Wilson coefficients $C_i(M_W)$ $i = 1, \dots, 10$ at the NLO level and C_g at the LO level can be written as

$$C_1(M_W) = 1 - \frac{11}{6} \frac{\alpha_s(M_W)}{4\pi} - \frac{35}{18} \frac{\alpha_{em}}{4\pi}, \quad (4)$$

$$C_2(M_W) = \frac{11}{2} \frac{\alpha_s(M_W)}{4\pi}, \quad (5)$$

$$\begin{aligned} C_3(M_W) &= -\frac{\alpha_s(M_W)}{24\pi} \left[E_0(x_t) + E_0^{NP} - \frac{2}{3} \right] \\ &\quad + \frac{\alpha_{em}}{6\pi} \frac{1}{\sin^2 \theta_W} \left[2B_0(x_t) + C_0(x_t) + C_0^{NP} \right], \end{aligned} \quad (6)$$

$$C_4(M_W) = \frac{\alpha_s(M_W)}{8\pi} \left[E_0(x_t) + E_0^{NP} - \frac{2}{3} \right], \quad (7)$$

$$C_5(M_W) = -\frac{\alpha_s(M_W)}{24\pi} \left[E_0(x_t) + E_0^{NP} - \frac{2}{3} \right], \quad (8)$$

$$C_6(M_W) = \frac{\alpha_s(M_W)}{8\pi} \left[E_0(x_t) + E_0^{NP} - \frac{2}{3} \right], \quad (9)$$

$$C_7(M_W) = \frac{\alpha_{em}}{6\pi} \left[4C_0(x_t) + 4C_0^{NP} + D_0(x_t) + D_0^{NP} - \frac{4}{9} \right], \quad (10)$$

$$C_8(M_W) = C_{10}(M_W) = 0, \quad (11)$$

¹For more details about the structure of model III and the available experimental constraints, one can see Refs. [14,2,17].

$$C_9(M_W) = \frac{\alpha_{em}}{6\pi} \left\{ 4C_0(x_t) + 4C_0^{NP} + D_0(x_t) + D_0^{NP} - \frac{4}{9} + \frac{1}{\sin^2 \theta_W} [10B_0(x_t) - 4C_0(x_t) + 4C_0^{NP}] \right\}, \quad (12)$$

$$C_g(M_W) = -\frac{1}{2} (E'_0(x_t) + E'^{NP}_0), \quad (13)$$

where $x_t = m_t^2/M_W^2$, the functions $B_0(x)$, $C_0(x)$, $D_0(x)$, $E_0(x)$ and E'_0 are the familiar Inami-Lim functions which describe the contributions from the W -penguin and Box diagrams in the SM, and can be found easily, for example, in Ref. [15]. The functions C_0^{NP} , D_0^{NP} , E_0^{NP} and E'^{NP}_0 in Eq.(13) describe the new physics contributions to Wilson coefficients in model III [11],

$$C_0^{NP} = \frac{-x_t}{16} \left[\frac{y_t}{1-y_t} + \frac{y_t}{(1-y_t)^2} \ln[y_t] \right] \cdot |\lambda_{tt}|^2, \quad (14)$$

$$D_0^{NP} = -\frac{1}{3} H(y_t) |\lambda_{tt}|^2, \quad (15)$$

$$E_0^{NP} = -\frac{1}{2} I(y_t) |\lambda_{tt}|^2, \quad (16)$$

$$E'_0^{NP} = \frac{1}{6} J(y_t) |\lambda_{tt}|^2 - K(y_t) |\lambda_{tt} \lambda_{bb}| e^{i\theta}, \quad (17)$$

with

$$H(y) = \frac{38y - 79y^2 + 47y^3}{72(1-y)^3} + \frac{4y - 6y^2 + 3y^4}{12(1-y)^4} \ln[y], \quad (18)$$

$$I(y) = \frac{16y - 29y^2 + 7y^3}{36(1-y)^3} + \frac{2y - 3y^2}{6(1-y)^4} \log[y], \quad (19)$$

$$J(y) = \frac{2y + 5y^2 - y^3}{4(1-y)^3} + \frac{3y^2}{2(1-y)^4} \log[y], \quad (20)$$

$$K(y) = \frac{-3y + y^2}{4(1-y)^2} - \frac{y}{2(1-y)^3} \log[y], \quad (21)$$

where $x_t = m_t^2/M_W^2$, $y_t = m_t^2/M_{H^+}^2$, and the small terms proportional to m_b^2/m_t^2 have been neglected.

Since the heavy charged Higgs bosons appeared in model III have been integrated out at the scale M_W , the QCD running of the Wilson coefficients $C_i(M_W)$ down to the scale $\mu = O(m_b)$ after including the NP contributions will be the same as in the SM. In the NDR scheme, by using the input parameters as given in Eqs.(3) and (27) and setting $\mu = 2.5$ GeV, we find that:

$$\begin{aligned} C_1 &= 1.1245, & C_2 &= -0.2662, & C_3 &= 0.0186, & C_4 &= -0.0458, \\ C_5 &= 0.0113, & C_6 &= -0.0587, & C_7 &= 0.0006, & C_8 &= 0.0007, \\ C_9 &= -0.0096, & C_{10} &= 0.0026, & C_g^{eff} &= 0.3364 \end{aligned} \quad (22)$$

where $C_g^{eff} = C_{8G} + C_5$.

In this letter, the generalized factorization ansatz as being used in Ref. [8] will be employed. For the studied seven B meson decay modes, we use the decay amplitudes as given in Ref. [7] without further discussion about details. We focus on estimating the new physics effects on these seven measured decay modes. In the NDR scheme and for $SU(3)_C$, the effective Wilson coefficients can be written as [8]

$$C_i^{eff} = \left[1 + \frac{\alpha_s}{4\pi} \left(\hat{r}_V^T + \gamma_V^T \log \frac{m_b}{\mu} \right) \right]_{ij} C_j + \frac{\alpha_s}{24\pi} A'_i (C_t + C_p + C_g) + \frac{\alpha_{ew}}{8\pi} B'_i C_e , \quad (23)$$

where $A'_i = (0, 0, -1, 3, -1, 3, 0, 0, 0, 0, 0)^T$, $B'_i = (0, 0, 0, 0, 0, 0, 1, 0, 1, 0)^T$, the matrices \hat{r}_V and γ_V contain the process-independent contributions from the vertex diagrams. The matrix γ_V and \hat{r}_V have been given explicitly, for example, in Eq.(2.17) and (2.18) of Ref. [8]². The function C_t , C_p , and C_g describe the contributions arising from the penguin diagrams of the current-current $Q_{1,2}$, the QCD operators Q_3-Q_6 , and the tree-level diagram of the magnetic dipole operator Q_{8G} , respectively. The explicit expressions of the functions C_t , C_p , and C_g can be found for example in Refs. [8,11]. We here also follow the procedure of Ref. [18] to include the contribution of magnetic gluon penguin.

In the generalized factorization ansatz, the effective Wilson coefficients C_i^{eff} will appear in the decay amplitudes in the combinations,

$$a_{2i-1} \equiv C_{2i-1}^{eff} + \frac{C_{2i}^{eff}}{N_c^{eff}}, \quad a_{2i} \equiv C_{2i}^{eff} + \frac{C_{2i-1}^{eff}}{N_c^{eff}}, \quad (i = 1, \dots, 5) \quad (24)$$

where the effective number of colors N_c^{eff} is treated as a free parameter varying in the range of $2 \leq N_c^{eff} \leq \infty$, in order to model the non-factorizable contribution to the hadronic matrix elements. It is evident that the reliability of generalized factorization approach has been improved since the effective Wilson coefficients C_i^{eff} appeared in Eq.(24) are now gauge invariant and infrared safe [19]. Although N_c^{eff} can in principle vary from channel to channel, but in the energetic two-body hadronic B meson decays, it is expected to be process insensitive as supported by the data [8].

In the B rest frame, the branching ratios $\mathcal{B}(B \rightarrow PP)$ can be written as

$$\mathcal{B}(B \rightarrow XY) = \frac{1}{\Gamma_{tot}} \frac{|p|}{8\pi M_B^2} |M(B \rightarrow XY)|^2 , \quad (25)$$

where $\Gamma_{tot}(B_u^-) = 3.982 \times 10^{-13}$ GeV and $\Gamma_{tot}(B_d^0) = 4.252 \times 10^{-13}$ GeV obtained by using $\tau(B_u^-) = 1.653 ps$ and $\tau(B_d^0) = 1.548 ps$ [20], p_B is the four-momentum of the B meson, $M_B = 5.279$ GeV is the mass of B_u or B_d meson, and

$$|p| = \frac{1}{2M_B} \sqrt{[M_B^2 - (M_X + M_Y)^2][M_B^2 - (M_X - M_Y)^2]} \quad (26)$$

is the magnitude of momentum of particle X and Y in the B rest frame.

In the numerical calculations the following input parameters will be used:

²The correct value of the element $(\hat{r}_{NDR})_{66}$ and $(\hat{r}_{NDR})_{88}$ should be 17 instead of 1 as pointed in Ref. [10].

- The coupling constants, gauge boson masses, light meson masses, \dots , (all masses in unit of GeV) [7,20]

$$\begin{aligned} \alpha_{em} &= 1/128, \alpha_s(M_Z) = 0.118, \sin^2 \theta_W = 0.23, G_F = 1.16639 \times 10^{-5} (GeV)^{-2}, \\ M_Z &= 91.188, M_W = 80.42, m_{B_d^0} = m_{B_u^\pm} = 5.279, m_{\pi^\pm} = 0.140, \\ m_{\pi^0} &= 0.135, m_\eta = 0.547, m_{\eta'} = 0.958, m_{K^\pm} = 0.494, m_{K^0} = 0.498. \end{aligned} \quad (27)$$

- The elements of CKM matrix in the Wolfenstein parametrization: $A = 0.81$, $\lambda = 0.2205$, $\rho = 0.12$ and $\eta = 0.34$ (which corresponds to $\gamma = 71^\circ$ and $\beta = 26^\circ$), and the uncertainty of $\delta\eta = \pm 0.08$ will be considered.
- We firstly treat the internal quark masses in the loops as constituent masses,

$$m_b = 4.88 GeV, m_c = 1.5 GeV, m_s = 0.5 GeV, m_u = m_d = 0.2 GeV. \quad (28)$$

Secondly, we use the current quark masses for m_i ($i = u, d, s, c, b$) which appear through the equation of motion when working out the hadronic matrix elements. For $\mu = 2.5 GeV$, one finds [7]

$$m_b = 4.88 GeV, m_c = 1.5 GeV, m_s = 0.122 GeV, m_d = 7.6 MeV, m_u = 4.2 MeV. \quad (29)$$

For the mass of heavy top quark we also use $m_t = \overline{m}_t(m_t) = 168 GeV$.

- The decay constants of light mesons (in the units of MeV) are

$$\begin{aligned} f_\pi &= 133, f_K = 158, f_\eta^u = f_\eta^d = 78, f_{\eta'}^u = f_{\eta'}^d = 68, \\ f_\eta^c &= -0.9, f_{\eta'}^c = -0.23, f_\eta^s = -113, f_{\eta'}^s = 141. \end{aligned} \quad (30)$$

where $f_{\eta'}^u$ and $f_{\eta'}^s$ have been defined in the two-angle-mixing formalism with $\theta_0 = -9.1^\circ$ and $\theta_8 = -22.2^\circ$ [21].

- The form factors at the zero momentum transfer are

$$F_0^{B\pi}(0) = 0.33, F_0^{BK}(0) = 0.38, F_0^{B\eta}(0) = 0.145, F_0^{B\eta'}(0) = 0.135 \quad (31)$$

in the BSW model [16], and

$$F_0^{B\pi}(0) = 0.36, F_0^{BK}(0) = 0.41, F_0^{B\eta}(0) = 0.16, F_0^{B\eta'}(0) = 0.145, \quad (32)$$

in the LQQSR approach [7]. Here the relation between $F_0^{B\eta'}(0)$ and $F_0^{B\pi}(0)$ as defined in Eq.(A12) in Ref. [7] has been used. The momentum dependence of $F_0(k^2)$ as defined in Ref. [16] is $F_0(k^2) = F_0(0)/(1 - k^2/m^2(0^+))$. The pole masses being used to evaluate the k^2 -dependence of form factors are $m(0^+) = 5.73$ GeV for $\bar{u}b$ and $\bar{d}b$ currents, and $m(0^+) = 5.89$ GeV for $\bar{s}b$ currents.

For the seven studied B meson decay modes, currently available measurements from CLEO, BaBar and Belle Collaboration [3–6] are as follows:

$$\mathcal{B}(B \rightarrow \pi^+ \pi^-) = \begin{cases} (4.3_{-1.5}^{+1.6} \pm 0.5) \times 10^{-6} & [\text{CLEO}], \\ (9.3_{-2.1}^{+2.8} \pm 1.2) \times 10^{-6} & [\text{BaBar}], \end{cases} \quad (33)$$

$$\mathcal{B}(B \rightarrow K^+ \pi^0) = \begin{cases} (11.6_{-2.7}^{+3.0} \pm 1.4) \times 10^{-6} & [\text{CLEO}], \\ (18.8_{-4.9}^{+5.5} \pm 2.3) \times 10^{-6} & [\text{Belle}], \end{cases} \quad (34)$$

$$\mathcal{B}(B \rightarrow K^+ \pi^-) = \begin{cases} (17.2_{-2.4}^{+2.5} \pm 1.2) \times 10^{-6} & [\text{CLEO}], \\ (12.5_{-2.6}^{+3.0} \pm 1.3) \times 10^{-6} & [\text{BaBar}], \\ (17.4_{-4.6}^{+5.1} \pm 3.4) \times 10^{-6} & [\text{BELLE}], \end{cases} \quad (35)$$

$$\mathcal{B}(B \rightarrow K^0 \pi^+) = (18.2_{-4.0}^{+4.6} \pm 1.6) \times 10^{-6} \quad [\text{CLEO}], \quad (36)$$

$$\mathcal{B}(B \rightarrow K^0 \pi^0) = \begin{cases} (14.6_{-5.1}^{+5.9} \pm 2.4) \times 10^{-6} & [\text{CLEO}], \\ (21_{-7.8}^{+9.3} \pm 2.5) \times 10^{-6} & [\text{BELLE}], \end{cases} \quad (37)$$

$$\mathcal{B}(B \rightarrow K^+ \eta') = \begin{cases} (80_{-9}^{+10} \pm 7) \times 10^{-6} & [\text{CLEO}], \\ (62 \pm 18 \pm 8) \times 10^{-6} & [\text{BaBar}], \end{cases} \quad (38)$$

$$\mathcal{B}(B \rightarrow K^0 \eta') = (89_{-16}^{+18} \pm 9) \times 10^{-6} \quad [\text{CLEO}]. \quad (39)$$

The measurements of CLEO, BaBar and BELLE Collaboration are consistent with each other within errors.

In Table I, we present the theoretical predictions of the branching ratios for the seven B decay modes in the framework of the SM and model III by using the form factors from Bauer, Stech and Wirbel (BSW) model [16] and Lattice QCD/QCD sum rule (LQQSR) model [22], as listed in the first and second entries respectively. The last column shows the CLEO data of $B \rightarrow K^0 \pi^+, K^0 \eta'$ decays, and the average of CLEO, BaBar and/or BELLE measurements for other five decay modes. Theoretical predictions are made by using the central values of input parameters as given in Eqs.(3,27-32), and assuming $M_{H^+} = 200\text{GeV}$ and $N_c^{eff} = 2, 3, \infty$ in the generalized factorization approach. The branching ratios collected in Table I are the averages of the branching ratios of B and anti- B decays. The ratio $\delta\mathcal{B}$ describes the new physics correction on the decay ratio and is defined as

$$\delta\mathcal{B}(B \rightarrow XY) = \frac{\mathcal{B}(B \rightarrow XY)^{III} - \mathcal{B}(B \rightarrow XY)^{SM}}{\mathcal{B}(B \rightarrow XY)^{SM}} \quad (40)$$

The last column in shows the CLEO data of $B \rightarrow K^0 \pi^+, K^0 \eta'$ decays, and the average of CLEO, BaBar and/or BELLE measurements for remaining four decay modes.

From Table I, we find that

- The SM prediction of $B^0 \rightarrow \pi^+ \pi^-$ decay is clearly much larger than the CLEO measurement, but agree with BaBar measurement. The new physics contribution to this tree-dominated decay mode, however, is negligibly small.
- For four $B \rightarrow K\pi$ decays, the SM predictions agree with experimental measurements within errors. In model III, the new physics enhancements are large in magnitude: $\sim 50\%$ *w.r.t* the SM predictions. The model III predictions are generally larger than the data for $B \rightarrow K^+ \pi, K^0 \pi^+$ decays but still agree with the data within 2σ errors since both the theoretical and experimental errors are still large now.

- For $B \rightarrow K\eta'$ decays, the new physics enhancements in model III are large in magnitude: $\sim 60\%$ *w.r.t* the SM predictions. Such enhancement can make the theoretical predictions become consistent with the CLEO/BaBar data within one standard deviation, as illustrated in Fig.1 where the dot-dashed and solid curve shows the theoretical prediction in the model III for $N_c^{eff} = 3, \infty$, respectively.
- Since the form factors in LQQSR approach are larger than those in the BSW model, the theoretical predictions in the LQQSR approach are generally larger than those in the BSW model by $\sim 15\%$.

Because the branching ratios of the studied B decay modes strongly depend on the values of involved form factors $F_0^{B\pi}(0)$, $F_0^{BK}(0)$ and $F_0^{B\eta'}(0)$, any information about these form factors from data will help us to refine the theoretical predictions. Since the $B^0 \rightarrow \pi^+\pi^-$ decay is a tree-dominated decay mode and the possible new physics effect is also negligibly small, the experimental measures of this decay lead to a stringent constraint on the form factor $F_0^{B\pi}(0)$. If we take the average of CLEO and BaBar measurements,

$$\mathcal{B}(B_d^0 \rightarrow \pi^+\pi^-) = (5.5 \pm 1.5) \times 10^{-6}, \quad (41)$$

as the experimental result, then the constraint on $F_0^{B\pi}(0)$ will be

$$F_0^{B\pi}(0) = 0.25 \pm 0.03 \quad (42)$$

by setting $A = 0.2205$, $\lambda = 0.81$, $\rho = 0.12$, $\eta = 0.34$, $N_c^{eff} = 3$, and by neglecting FSI also.

Theoretically, small form factor $F_0^{B\pi}(0)$ will lead to small predicted branching ratios of $B \rightarrow K\pi$ and $B \rightarrow K\eta'$ decays. First, the relation between $F_0^{B\eta'}(0)$ and $F_0^{B\pi}(0)$ as given in Ref. [7] is

$$F_0^{B\eta'}(0) = F_0^{B\pi}(0)(\sin \theta_8/\sqrt{6} + \cos \theta_0/\sqrt{3}) \quad (43)$$

with $\theta_0 = -9, 1^\circ$ and $\theta_8 = -22.2^\circ$. A small $F_0^{B\pi}(0)$ leads to a small $F_0^{B\eta'}$ and in turn small branching ratios of $B \rightarrow K\eta'$ decays. Second, $F_0^{BK}(0)$ cannot deviate too much from $F_0^{B\pi}(0)$, otherwise the $SU(3)$ -symmetry relation $F_0^{B\pi} \approx F_0^{BK}$ will be badly broken. In Table II, we show the branching ratios of seven studied decay modes obtained by using $F_0^{B\pi}(0) = 0.25$ instead of 0.33 while keep all other input parameters remain the same as being used in Table I.

Contrary to the case of using $F_0^{B\pi}(0) = 0.33$ in the BSW model, where the inclusion of new physics contributions in the model III will degenerate the agreement between the theoretical predictions and the data for first three $B \rightarrow K\pi$ decay modes, the inclusion of $\sim 50\%$ new physics enhancements to $B \rightarrow K\pi$ decays for the case of using $F_0^{B\pi}(0) = 0.25$ does improve the agreement between the theory and the data, as illustrated in Figs.(2,3) where the short-dashed and solid curve shows the predictions in the SM and model III for the case of using $F_0^{B\pi}(0) = 0.25$. The horizontal band between two dots lines corresponds to the (averaged) data with 2σ errors.

For the decay $B \rightarrow K^0\pi^0$ we find $\mathcal{B}(B \rightarrow K^0\pi^0) = (4.3 \pm 2.1) \times 10^{-6} \times (F_0^{B\pi}(0)/0.25)^2$ in the SM, which is almost four times smaller than the central value of the averaged data: $\mathcal{B}(B \rightarrow K^0\pi^0) = (16.6 \pm 5.3) \times 10^{-6}$. The sixty percent new physics enhancement will be

helpful to increase the theoretical prediction, but is still not large enough to cover the gap, as illustrated in Fig.(3b) where the lower short-dashed and solid curves show the theoretical prediction in the SM and model III with $F_0^{B\pi}(0) = 0.25$. This problem will become clear when more precise data from B factories are available.

For $F_0^{B\pi}(0) = 0.25$, the SM predictions for branching ratios of $B \rightarrow K\eta'$ decays are in the range of $(18 - 40) \times 10^{-6}$ as shown in Table II and clearly much smaller than the data. We know that the $K\eta'$ decay rates can be enhanced, for example, through (i) constructive interference in gluonic penguin diagrams, which is qualitatively OK but numerical problems remain; (ii) the small running mass m_s at the scale m_b ³; (iii) larger form factor $F_0^{B\eta'}(0)$ due to the smaller $\eta - \eta'$ mixing angle -15.4^0 rather than $\approx -20^0$; (iv) contribution from the intrinsic charm content of η' [23]. However, as pointed out in Ref. [18], the above mentioned enhancement is partially washed out by the anomaly effects in the matrix element of pseudo-scalar densities, an effect overlooked before. As a consequence, the net enhancement may be not large enough. For a smaller $F_0^{B\pi}(0) = 0.25 \pm 0.03$ preferred by the data, the discrepancy between the data and the SM predictions for $B \rightarrow K\eta'$ decays becomes larger.

In the model III, however, the new gluonic and electroweak penguin diagrams contribute to the $B \rightarrow K^+\eta'$ and $K^0\eta'$ decays through constructive interference with their SM counterparts and consequently provide the large enhancements, $\sim 60\%$ *w.r.t.* the SM predictions, to make the theoretical predictions become consistent with the data even for $F_0^{B\pi}(0) = 0.25$ instead of 0.33 as shown in Table II and Fig.4.

In Fig.4, we plot the mass-dependence of $\mathcal{B}(B^+ \rightarrow K^+\eta')$ and $\mathcal{B}(B^0 \rightarrow K^0\eta')$ in the SM and model III by using $F_0^{B\pi}(0) = 0.25$ instead of 0.33 (while all other input parameters are the same as in Fig.1). The short-dashed line in Fig.4 shows the SM predictions with $N_c^{eff} = 3$. The dot-dashed and solid curve refer to the branching ratios in the model III for $N_c^{eff} = 3$ and ∞ , respectively. The upper dots band corresponds to the data with 2σ errors: $\mathcal{B}(B \rightarrow K^+\eta') = (75 \pm 20) \times 10^{-6}$ and $\mathcal{B}(B \rightarrow K^0\eta') = (89^{+40}_{-36}) \times 10^{-6}$.

By comparing the curves in Fig.1 and Fig.4, it is easy to see that (a) the gap between the SM predictions of $B \rightarrow K\eta'$ decay rates and the data is enlarged by using $F_0^{B\pi}(0) = 0.25$ instead of 0.33; (b) the new physics enhancement therefore becomes essential for the theoretical predictions to be consistent with CLEO/BaBar result within one standard deviation.

We know that the calculation of charmless hadronic B meson decay rates suffers from many theoretical uncertainties [7,8]. Most of them have been considered in our calculation. If we consider effects induced by the uncertainties of major input parameters $\eta = 0.34 \pm 0.08$, $k^2 = m_b^2/2 \pm 2$ GeV 2 , $F_0^{B\pi}(0) = 0.25 \pm 0.03$, $F_0^{BK}(0) = 0.30 \pm 0.05$, $0 \leq 1/N_c^{eff} \leq 0.5$, $M_{H^+} = 200 \pm 100$ GeV and $m_s = 0.1 - 0.122$ GeV, we find numerically that

$$\mathcal{B}(B \rightarrow K^+\eta') \approx \mathcal{B}(B \rightarrow K^0\eta') = \begin{cases} (17 - 50) \times 10^{-6} & \text{in SM,} \\ (28 - 75) \times 10^{-6} & \text{in model III.} \end{cases} \quad (44)$$

The SM prediction of $B \rightarrow K\eta'$ is much smaller than the data, while the model III prediction can be consistent with the data within one standard deviation. This is a simple and plausible new physics interpretation for the observed $\eta'K$ puzzle.

³However, a rather small m_s is not consistent with recent lattice calculations.

As simple illustrations we show explicitly the dependence of the branching ratios $\mathcal{B}(B \rightarrow K\eta')$ on the form factor $F_0^{BK}(0)$ and the running quark mass m_s in Figs.(5,6). In Fig.5, we plot the $F_0^{BK}(0)$ dependence of the ratios $\mathcal{B}(B \rightarrow K^+\eta')$ and $\mathcal{B}(B \rightarrow K^0\eta')$ in the SM and model III, assuming $M_{H^+} = 200$ GeV, $F_0^{B\pi}(0) = 0.25$ and $F_0^{BK}(0) = 0.25 - 0.40$. The short-dashed line shows the SM predictions with $N_c^{eff} = 3$. The dot-dashed and solid curve refer to the branching ratios in model III for $N_c^{eff} = 3$ and ∞ , respectively. The dots band corresponds to the (averaged) data with 2σ errors. The theoretical predictions also show a strong dependence upon $F_0^{BK}(0)$: $\mathcal{B}(B \rightarrow K^+\eta') = 13.8 \times 10^{-6}$ and 26.3×10^{-6} in the SM for $N_c^{eff} = 3$ and $F_0^{BK}(0) = 0.25$ and 0.40 , respectively.

In Fig.6, we plot the m_s -dependence of the ratios $\mathcal{B}(B \rightarrow K^+\eta')$ and $\mathcal{B}(B \rightarrow K^0\eta')$ in the SM and model III with $F_0^{B\pi}(0) = 0.25$, $F_0^{BK}(0) = 0.33$ and $M_{H^+} = 200$ GeV. The short-dashed line shows the SM predictions with $N_c^{eff} = 3$. The dot-dashed and solid curve refer to the branching ratios in model III for $N_c^{eff} = 3$ and ∞ , respectively. The dots band corresponds to the (averaged) data with 2σ errors. The theoretical predictions show a very strong dependence upon the mass m_s : $\mathcal{B}(B \rightarrow K^+\eta') = 44.8 \times 10^{-6}$ and 18.6×10^{-6} in the SM for $N_c^{eff} = 3$ and $m_s = 0.08$ GeV and 0.15 GeV, respectively.

In short, we here studied the new physics contributions to the seven observed $B \rightarrow PP$ decay modes, and made an effort to find a new physics interpretation for the so-called $\eta'K$ puzzle of B meson decays by employing the effective Hamiltonian with generalized factorization. Within the considered parameter space we found that:

- The new physics enhancement is negligibly small to tree-dominated $B \rightarrow \pi^+\pi^-$ decay, but can be significant to the penguin-dominated $B \rightarrow K\pi$ and $B \rightarrow K\eta'$ decay modes, $\sim (40 - 70)\%$ *w.r.t* the SM predictions.
- The CLEO/BaBar measurement of $B \rightarrow \pi^+\pi^-$ decay prefers a small $F_0^{B\pi}(0)$: $F_0^{B\pi}(0) = 0.25 \pm 0.03$ instead of 0.33 or 0.36 in the BSW and LQQSR form factors. A smaller $F_0^{B\pi}(0)$ will leads to smaller predictions for other six $B \rightarrow K\pi$ and $B \rightarrow K\eta'$ decay modes studied here. The new physics enhancements to $B \rightarrow K\pi$ decays are helpful to improve the agreement between the data and theoretical predictions for these decays.
- The new physics enhancements can boost the theoretical predictions of the branching ratios $\mathcal{B}(B \rightarrow K^+\eta')$ and $\mathcal{B}(B \rightarrow K^0\eta')$ to be consistent with the data within one standard deviation. This is a simple and plausible new physics interpretation for the observed $\eta'K$ puzzle.

ACKNOWLEDGMENTS

C.S. Li and K.T. Chao acknowledge the support by the National Natural Science Foundation of China, the State Commission of Science and technology of China and the Doctoral Program Foundation of Institution of Higher Education. Z.J. Xiao acknowledges the support by the National Natural Science Foundation of China under the Grant No.19575015 and 10075013, and by the Excellent Young Teachers Program of Ministry of Education, P.R.China.

REFERENCES

- [1] P.F. Harrison and H.R. Quinn, Editors, *The BaBar Physics Book*, SLAC-R-504, 1998; R. Fleischer and J. Matias, Phys.Rev.**D61**, 074004(2000).
- [2] Z.J. Xiao, C.S. Li and K.T. Chao, Phys.Lett. **B473**, 148(2000); Z.J. Xiao, C.S. Li and K.T. Chao, Phys.Rev. **D62**, 094008(2000).
- [3] S.J. Richichi *et al.*, CLEO Collaboration, Phys.Rev.Lett. **85**, 520(2000);
- [4] D. Cronin-Hennessy *et al.*, CLEO Collaboration, Phys.Rev.Lett. **85**, 515(2000);
- [5] A. Gritsan, Talk presented at UCSB, UCSD, LBNL, SLAC, CU-Boulder, March-May 2000, CLEO TALK 00-20.
- [6] A. Abashian *et al.*, Belle Collaboration, talks given at ICHEP'2000, Osaka, Japan, 27 Jul - 2 Aug, 2000, Conf0005, Conf-0006, Conf0007;
- [7] A. Ali, G. Kramer and C.D. Lü, Phys.Rev. **D58**, 094009(1998).
- [8] Y.H. Chen, H.Y. Cheng, B. Tseng and K.C. Yang, Phys.Rev. **D60**, 094014(1999);
- [9] B.H. Behrens *et al.*, CLEO Collaboration, Phys.Rev.Lett. **80**, 3710(1998).
- [10] H.Y. Cheng and B. Tseng, Phys.Rev. **D62**, 054029(2000).
- [11] Z.J. Xiao, C.S. Li and K.T. Chao, hep-ph/0010326, to be published in Phys.Rev. D.
- [12] I. Halperin and A. Zhitnitsky, Phys.Rev.Lett. **80**, 438(1998); W.S. Hou and B. Tseng, Phys.Rev.Lett. **80**, 434(1998); D.S. Du, C.S. Kim and Y.D. Yang, Phys.Lett. **B426**, 133 (1998); H.Y. Cheng and B. Tseng, Phys.Rev. **D58**, 094005(1998);
- [13] T.P. Cheng and M. Sher, Phys.Rev. **D35**, 3484(1987); M. Sher and Y. Yuan, Phys.Rev. **D44**, 1461(1991); W.S. Hou, Phys.Lett. **B296**, 179(1992); A. Antaramian, L.J. Hall and A. Rasin, Phys. Rev. Lett. **69**, 1871 (1992); L.J. Hall and S. Winberg, Phys.Rev. **D48**, R979 (1993); D. Chang, W.S. Hou and W.Y. Keung, Phys.Rev. **D48**, 217 (1993); Y.L. Wu and L. Wolfenstein, Phys.Rev.Lett. **73**, 1762 (1994); D. Atwood, L. Reina and A. Soni, Phys.Rev. Lett. **75**, 3800 (1995); G. Cvetic, S.S. Hwang and C.S. Kim, Phys.Rev. **D58**, 116003(1998).
- [14] D. Atwood, L. Reina and A. Soni, Phys.Rev. **bf D55**, 3156 (1997).
- [15] For a review see G. Buchalla, A.J. Buras and M.E. Lautenbacher, Rev.Mod.Phys. **68**, 1125(1996).
- [16] M. Bauer and B. Stech, Phys.Lett. **B152**, 380 (1985);
M. Bauer, B. Stech and M. Wirbel, Z. Phys. **C29**, 637 (1985); ibid, **C34**, 103 (1987).
- [17] D.B. Chao, K. Cheung and W.Y. Keung, Phys.Rev. **D59**, 115006 (1999).
- [18] A. Ali, C. Greub, Phys.Rev. **D57**, 2996 (1998).
- [19] H.-Y. Cheng, Hsiang-nan Li and K.C. Yang, Phys.Rev. **D60**, 094005(1999).
- [20] Particle Data Group, D.E. Groom *et al.*, Eur. Phys. J. **C15**, 1(2000).
- [21] T. Feldmann and P. Kroll, Eur.Phys.J. **C5**, 327 (1998).
- [22] J.M. Flynn and C.T. Sachrajda, hep-lat/9710057, and reference therein.
- [23] F. Yuan and K.T. Chao, Phys.Rev. **D56**, 2495(1997); I. Halperin and A. Zhitnitsky, Phys.Rev. **D56**, 7247(1997); E.V. Shuryak and A. Zhitnitsky, Phys.Rev. **D57**, 2001(1998).

TABLES

TABLE I. Branching ratios (in units of 10^{-6}) of seven studied B decay modes in the SM and model III by using the BSW (the first entries) and LQQSR (the second entries) form factors, with $k^2 = m_b^2/2$, $A = 0.81$, $\lambda = 0.2205$, $\rho = 0.12$, $\eta = 0.34$, $\theta = 0^\circ$, $N_c^{eff} = 2, 3, \infty$ and $M_{H^+} = 200$ GeV. The last column shows the (averaged) data.

Channel	SM			Model III			$\delta\mathcal{B} [\%]$			Data
	2	3	∞	2	3	∞	2	3	∞	
$B^0 \rightarrow \pi^+ \pi^-$	9.03	10.3	12.9	9.26	10.5	13.2	2.5	2.5	2.4	5.5 ± 1.5
	10.7	12.2	15.4	11.0	12.5	15.8	2.5	2.5	2.4	
$B^+ \rightarrow K^+ \pi^0$	12.1	13.5	16.7	17.4	19.6	24.4	45	45	46	13.3 ± 2.9
	14.3	16.0	19.8	20.7	23.3	29.0	45	45	46	
$B^0 \rightarrow K^+ \pi^-$	17.7	19.6	23.8	26.6	29.7	36.3	51	51	53	15.9 ± 2.2
	21.0	23.3	28.3	31.7	35.3	43.1	51	51	53	
$B^+ \rightarrow K^0 \pi^+$	20.0	23.3	30.7	29.9	34.7	45.4	50	49	48	$18.2^{+4.9}_{-4.3}$
	23.8	27.7	36.5	35.6	41.3	54.0	50	49	48	
$B^0 \rightarrow K^0 \pi^0$	7.22	8.25	10.6	11.3	12.9	16.5	57	57	56	16.6 ± 5.3
	8.61	9.85	12.6	13.5	15.4	19.7	57	57	56	
$B^+ \rightarrow K^+ \eta'$	22.9	28.8	42.9	38.5	47.5	68.3	68	65	59	75 ± 10
	26.3	33.1	49.3	42.3	52.8	78.5	69	65	59	
$B^0 \rightarrow K^0 \eta'$	22.0	28.3	43.1	36.8	46.0	67.5	67	63	57	89^{+20}_{-18}
	25.3	32.4	49.5	42.3	52.8	77.6	67	63	57	

TABLE II. Branching ratios (in units of 10^{-6}) of seven studied B decay modes in the SM and Model III by using the BSW form factors with $F_0^{B\pi}(0) = 0.25$ instead of $F_0^{B\pi}(0) = 0.33$, and assuming $k^2 = m_b^2/2$, $A = 0.81$, $\lambda = 0.2205$, $\rho = 0.12$, $\eta = 0.34$, $N_c^{eff} = 2, 3, \infty$, $\theta = 0^\circ$ and $M_{H^+} = 200$ GeV. The last column shows the (averaged) data.

Channel	SM			Model III			$\delta\mathcal{B} [\%]$			Data
	2	3	∞	2	3	∞	2	3	∞	
$B^0 \rightarrow \pi^+ \pi^-$	5.18	5.89	7.42	5.31	6.03	7.60	2.5	2.5	2.4	5.5 ± 1.5
$B^+ \rightarrow K^+ \pi^0$	7.44	8.36	10.4	10.6	12.0	15.0	43	43	44	13.3 ± 2.9
$B^0 \rightarrow K^+ \pi^-$	10.1	11.2	13.6	15.3	17.0	20.8	51	51	53	15.9 ± 2.2
$B^+ \rightarrow K^0 \pi^+$	11.5	13.4	17.6	17.2	19.9	26.0	50	49	48	$18.2^{+4.9}_{-4.3}$
$B^0 \rightarrow K^0 \pi^0$	3.79	4.29	5.46	6.04	6.85	8.70	60	60	60	16.6 ± 5.3
$B^+ \rightarrow K^+ \eta'$	19.1	24.4	36.9	32.5	40.4	58.9	70	66	60	75 ± 10
$B^0 \rightarrow K^0 \eta'$	18.3	23.7	36.6	30.9	38.9	57.6	69	64	58	89^{+20}_{-18}

FIGURES

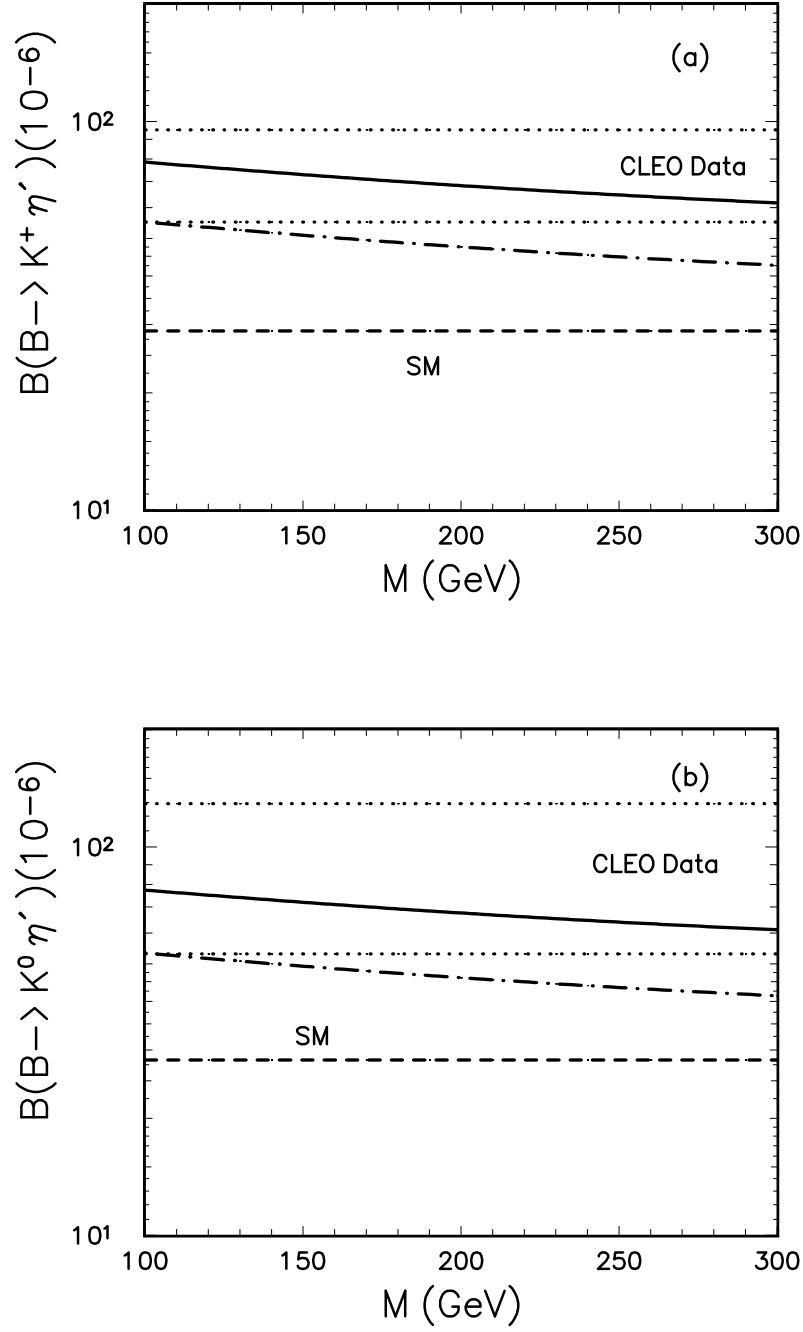


FIG. 1. Plots of branching ratios of decays $B^+ \rightarrow K^+ \eta'$ (1a) and $B^0 \rightarrow K^0 \eta'$ (1b) versus mass M_{H^+} in the SM and model III with $F_0^{B\pi}(0) = 0.33$. The short-dashed line shows the SM predictions with $N_c^{eff} = 3$. The dot-dashed and solid curve refers to the branching ratios in the model III for $N_c^{eff} = 3$ and ∞ , respectively. The dots band corresponds to the CLEO/BaBar data with 2σ errors.

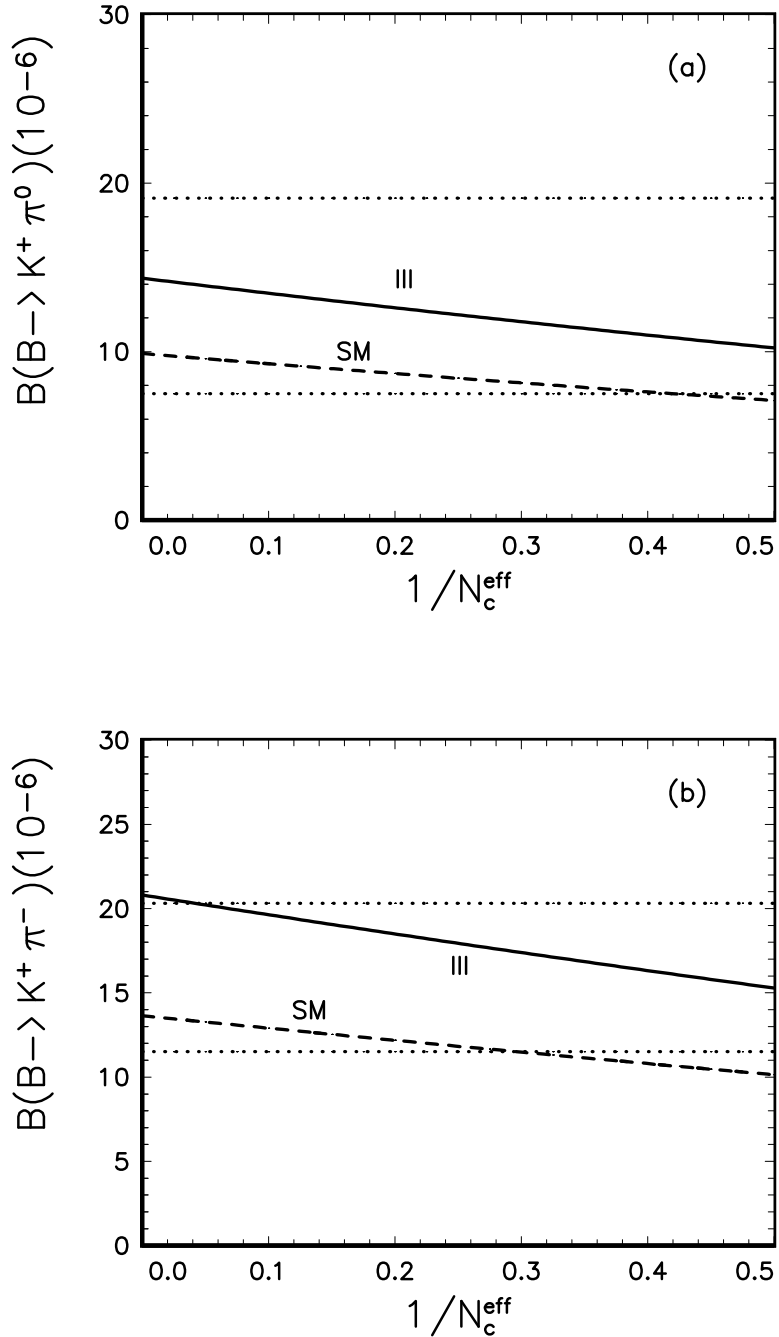


FIG. 2. Plots of branching ratios of decays $B \rightarrow K^+ \pi^0$ (2a) and $K^+ \pi^-$ (2b) versus $1/N_c^{\text{eff}}$ in the SM and model III assuming $M_{H^+} = 200$ GeV. The short-dashed and solid curve show the predictions in the SM and model III using $F_0^{B\pi}(0) = 0.25$. The dots band corresponds to the (averaged) data with 2σ errors.

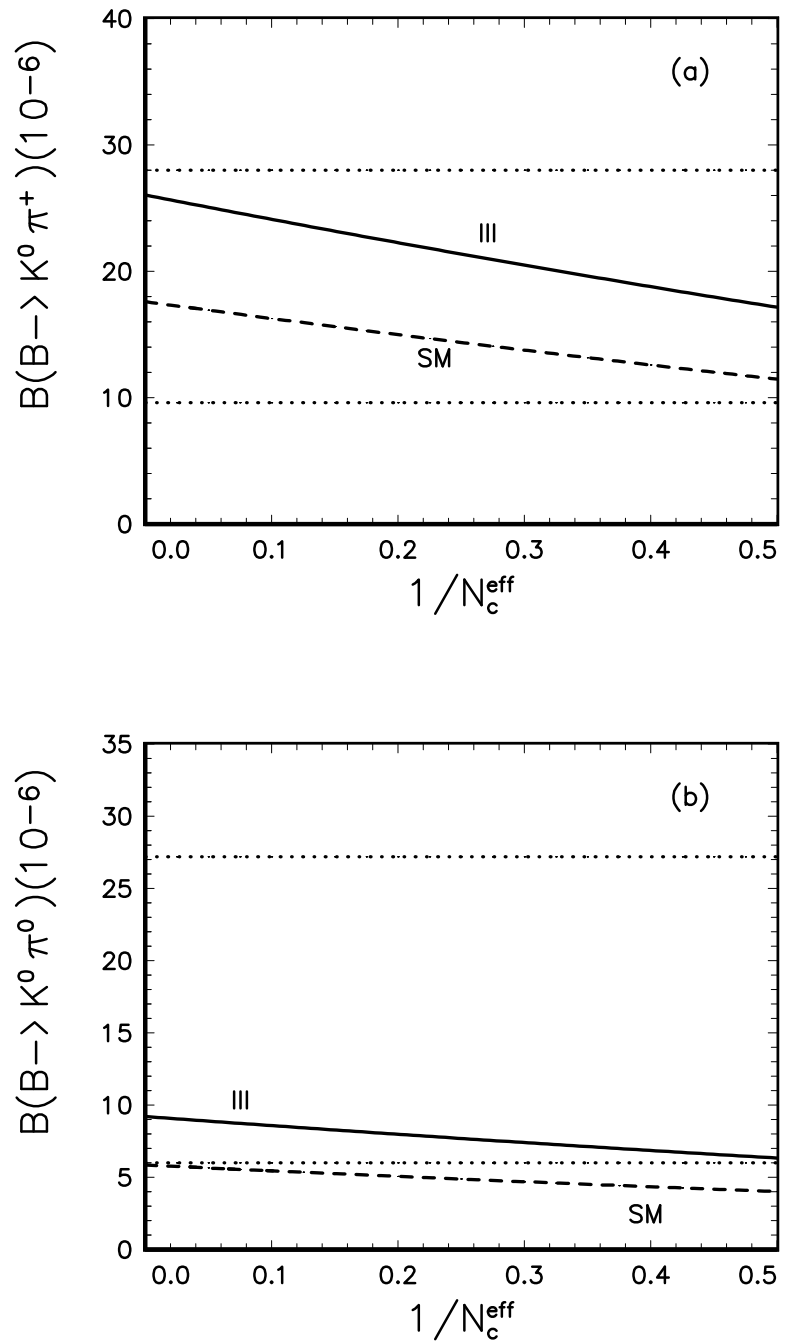


FIG. 3. Same as Fig.2 but for $B \rightarrow K^0 \pi^+$ (3a) and $K^0 \pi^0$ (3b) decay modes.

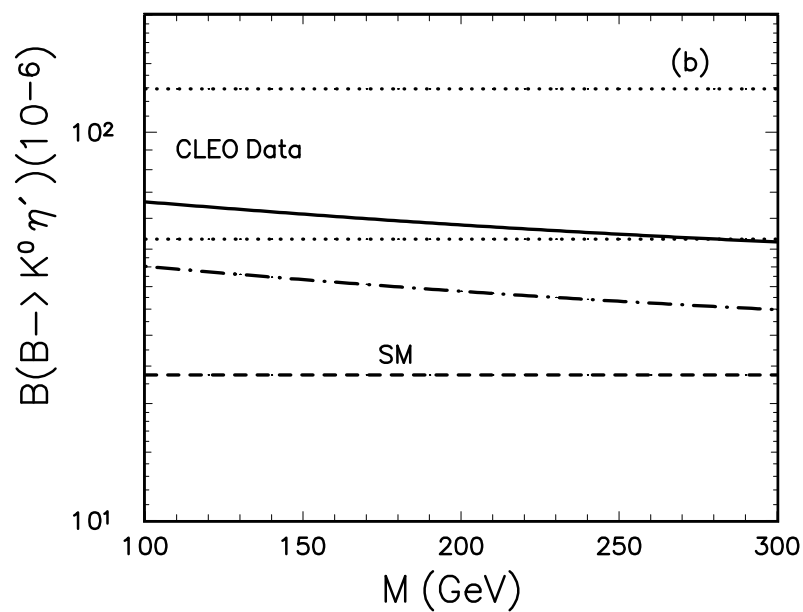
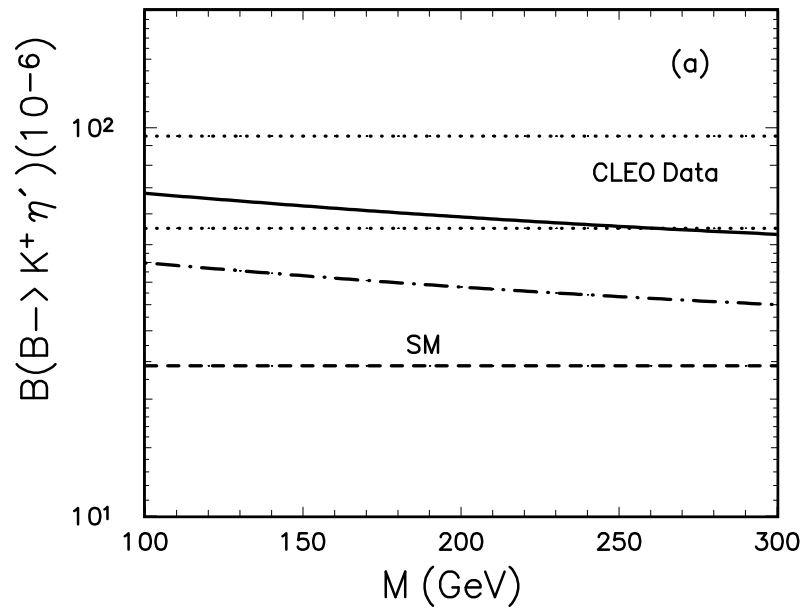


FIG. 4. Same as Fig.1 but for $F_0^{B\pi}(0) = 0.25$.

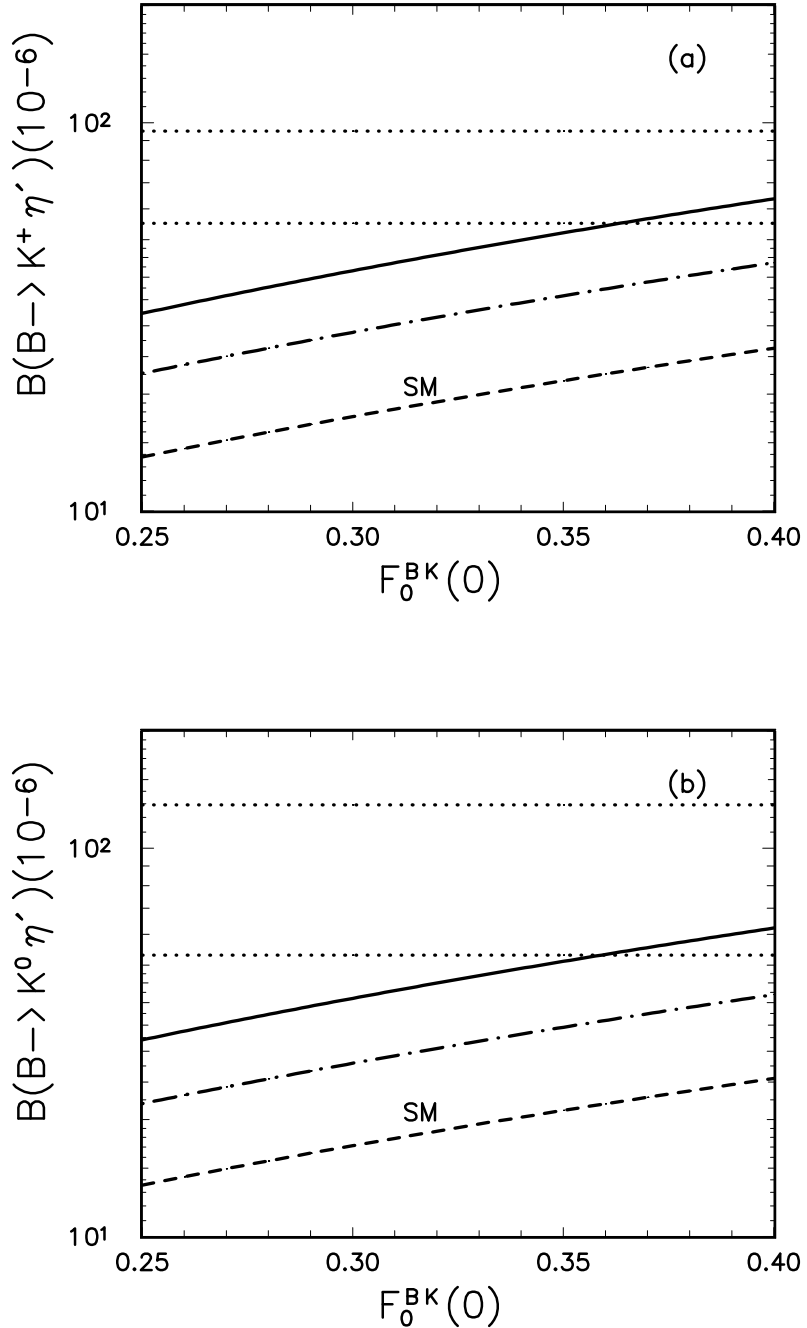


FIG. 5. Plots of branching ratios of decays $B^+ \rightarrow K^+ \eta'$ (5a) and $B^0 \rightarrow K^0 \eta'$ (5b) versus form factor $F_0^{BK}(0)$ in the SM and model III. The short-dashed line shows the SM predictions with $N_c^{eff} = 3$. The dot-dashed and solid curve refers to the branching ratios in the model III for $N_c^{eff} = 3$ and ∞ , respectively. The dots band corresponds to the (averaged) data with 2σ errors.

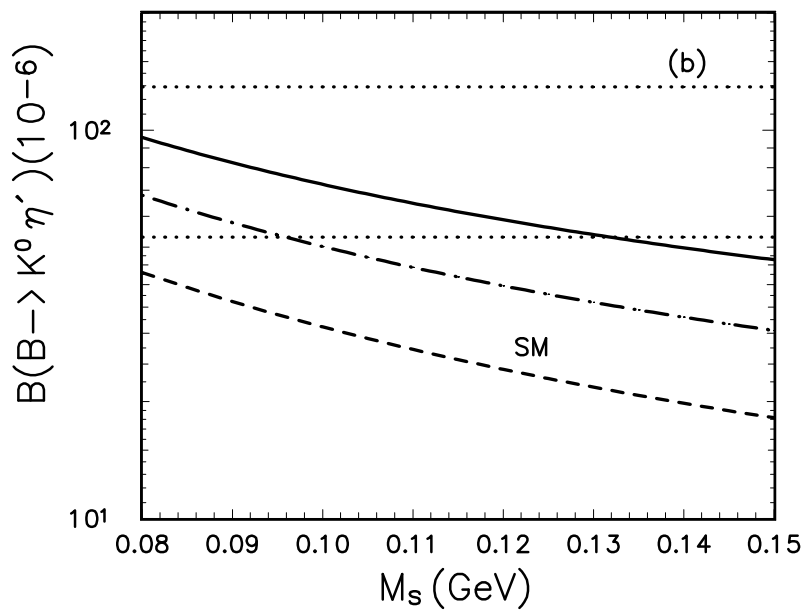
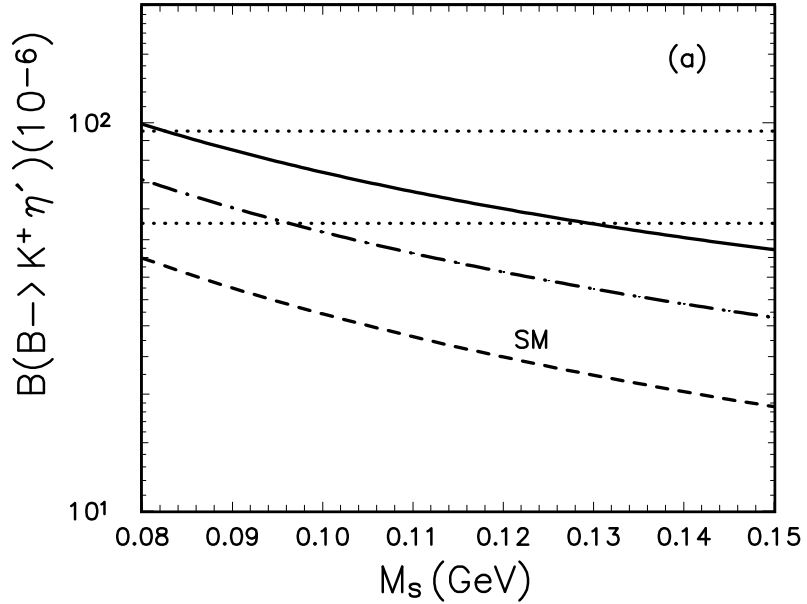


FIG. 6. Plots of branching ratios of decays $B^+ \rightarrow K^+ \eta'$ (6a) and $B^0 \rightarrow K^0 \eta'$ (6b) versus mass m_s in the SM and model III with $F_0^{B\pi} = 0.25$, $F_0^{BK} = 0.33$ and $M_{H^+} = 200$ GeV. The short-dashed line shows the SM predictions with $N_c^{eff} = 3$. The dot-dashed and solid curve refers to the branching ratios in the model III for $N_c^{eff} = 3$ and ∞ , respectively. The dots band corresponds to the (averaged) data with 2σ errors.